Intracellular Localization of Arabidopsis Sulfurtransferases[1]

Michael Bauer, Christof Dietrich, Katharina Nowak, Walter D. Sierralta, and Jutta Papenbrock*

Institute for Botany (M.B., J.P.) and Institute for Plant Diseases and Plant Protection (C.D.), University of Hannover, D–30419 Hannover, Germany; Institute for Plant Biology, Technical University of Braunschweig, D–38106, Braunschweig, Germany (K.N.); and Laboratory of Ultrastructures, INTA University of Chile, 5540 Macul Santiago, Chile (W.D.S.)

Sulfurtransferases (Str) comprise a group of enzymes widely distributed in archaea, eubacteria, and eukaryota which catalyze the transfer of a sulfur atom from suitable sulfur donors to nucleophilic sulfur acceptors. In all organisms analyzed to date, small gene families encoding Str proteins have been identified. The gene products were localized to different compartments of the cells. Our interest concerns the localization of Str proteins encoded in the nuclear genome of Arabidopsis. Computer-based prediction methods revealed localization in different compartments of the cell for six putative AtStrs. Several methods were used to determine the localization of the AtStr proteins experimentally. For AtStr1, a mitochondrial localization was demonstrated by immunodetection in the proteome of isolated mitochondria resolved by one- and two-dimensional gel electrophoresis and subsequent blotting. The respective mature AtStr1 protein was identified by mass spectrometry sequencing. The same result was obtained by transient expression of fusion constructs with the green fluorescent protein in Arabidopsis protoplasts, whereas AtStr2 was exclusively localized to the cytoplasm by this method. Three members of the single-domain AtStr were localized in the chloroplasts as demonstrated by transient expression of green fluorescent protein fusions in protoplasts and stomata, whereas the single-domain AtStr18 was shown to be cytoplasmic. The remarkable subcellular distribution of AtStr15 was additionally analyzed by transmission electron immunomicroscopy using a monospecific antibody against green fluorescent protein, indicating an attachment to the thylakoid membrane. The knowledge of the intracellular localization of the members of this multiprotein family will help elucidate their specific functions in the organism.

All members in the sulfurtransferase (Str)/rhodanese protein family in archaea, eubacteria, and eukaryota are unified by characteristic well-defined sequence domains (Bordo and Bork, 2002). These domains are found as tandem repeats, with the C-terminal domain containing the active site Cys residue, as single-domain proteins or as members of multidomain proteins (Bordo and Bork, 2002). The 18 proteins identified in Arabidopsis which contain at least one Str signature were classified into six groups on the basis of their sequence homology (Bauer and Papenbrock, 2002; http://arabidopsis.org/info/genefamily/STR_genefamily.html). Group I consists of two Str proteins with two-domain; the five proteins in group VI contain only the C-terminal Str signature and thus possess similarity to the single-domain Str from bacteria.

Strs catalyze the transfer of a sulfur atom from suitable sulfur donors to a nucleophilic acceptor. Specific biological roles for most members of this superfamily have not been established (Spallarossa et al., 2001). Proposed roles include cyanide detoxification (Vennesland et al., 1982), involvement in sulfate assimilation (Donadio et al., 1990), and mobilization of sulfur for iron-sulfur cluster biosynthesis or repair (Bonomi et al., 1977). The most studied and best characterized Str is bovine rhodanese (thiosulfate:cyanide Str, EC 2.8.1.1), which catalyzes in vitro the transfer of a sulfane sulfur atom from thiosulfate to cyanide, leading to the formation of sulfite and thiocyanate (Westley, 1973).

Strs have been identified in different compartments in living organisms. In *Escherichia coli,* seven Str proteins were identified; a single-domain Str, GlpE, is a cytoplasmic protein, whereas at least one two-domain Str was localized in the periplasm (Ray et al., 2000). In the cyanobacterium *Synechococcus* sp. strain PCC 7942, a rhodanese-like protein was localized to the periplasmic space and was suggested to play a role in the transport of specific sulfur compounds (Laudenbach et al., 1991). In mammalia two different Str enzymes with 3-mercaptopyruvate and thiosulfate-specific activities have been identified which are characterized by different K_m values for both substrates. The 3-mercaptopyruvate Str protein was localized by immunogold-labeling and western-blot analysis to the cytoplasm and the mitochondria, whereas thiosulfate Str was detected exclusively in mitochondria and mainly in liver cells. 3-mercaptopyruvate Str might detoxify cyanide in the cytoplasm, and in the mitochondria both Str enzymes would protect

[1] This work was supported by the Deutsche Forschungsgemeinschaft (projects PA764/1–3 to M.B. and J.P. and ME1266/14–2 to K.N) and by an EU funded research consortium in the VRTP-IMPACT project (C.D.).

* Corresponding author; e-mail jutta.papenbrock@botanik.uni-hannover.de; fax 49–511–762–3992.

cytochrome c oxidase effectively (Nagahara et al., 1995, 1999). The intracellular localization of Str1 and Str2 of Arabidopsis has been investigated previously (Hatzfeld and Saito, 2000; Nakamura et al., 2000; Papenbrock and Schmidt, 2000a); however the localization results obtained by fusion with the green fluorescent protein (GFP) were ambiguous. Recently, the single-domain Str protein, Ntdin from tobacco, a homolog of the AtStr15 protein from Arabidopsis with 56.8% identity, was localized in the chloroplasts by transient expression of GFP fusions (Yang et al., 2003), supporting the early report of the Str/rhodanese presence in the chloroplasts (Tomati et al., 1972).

Our aim of the research in this paper is the functional analysis of all members of the nuclear encoded Str multiprotein family in Arabidopsis. Knowledge of their intracellular localization is a prerequisite for the determination of their metabolic roles in multicellular organisms. Computer-based prediction programs are not yet sufficiently reliable and are only indicative of the in vivo localization of proteins. For exclusively immuno-based localization methods, many monospecific antibodies which are also difficult to produce against highly similar proteins would be required. The mitochondrial localization of AtStr1 was demonstrated by several different methods leading to the same conclusions. The transient expression of GFP fusion proteins in Arabidopsis protoplasts was established as a reliable method for the determination of the intracellular localization as confirmed by a number of controls.

RESULTS

Intracellular Localization of AtStr1 in Mitochondria

Arabidopsis protoplasts were transformed using a transient expression system with *AtStr1* and *AtStr2* including (wPS) or excluding (woPS) their putative targeting peptide sequences (Fig. 1; for an overview of the constructs see Table I). Colocalization of the AtStr1wPS/pGFP-N fluorescence with MitoTracker Orange fluorescence, a dye that is specifically enriched in mitochondria, in the same protoplasts using a confocal laser scanning microscope (CLSM) resulted in the same picture. A second control for mitochondrial intracellular localization was used: the targeting peptide of the mitochondrial protein, Ser hydroxymethyltransferase, was fused to the GFP protein, resulting in the same image as transient transformation with the AtStr1 fusion construct (data not shown). These results indicated import of the AtStr1 protein into the mitochondria (Fig. 1, A and B). The same localization results were obtained with a fluorescence microscope (Fig. 1D). The corresponding bright field picture visualizes the protoplast's cell membrane, demonstrates the intactness of the protoplasts, and demonstrates the position of the chloroplasts (Fig. 1C). *AtStr1* expressed without its putative targeting peptide sequence remained in the cytoplasm (Fig. 1F). The fusion

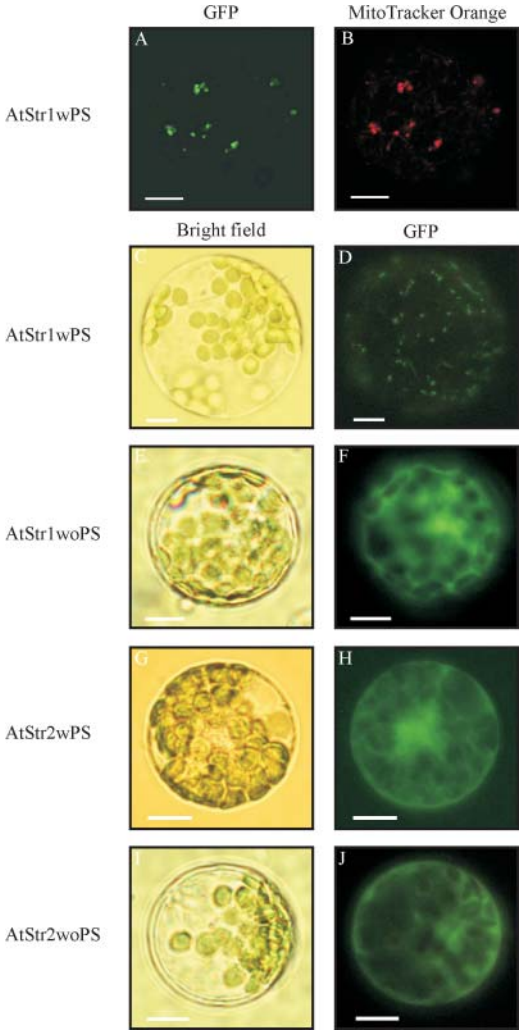

Figure 1. Subcellular localization of AtStr1 and AtStr2 GFP fusion constructs with and without signal peptide. A, Arabidopsis protoplasts were transformed with *AtStr1* including its targeting peptide sequence (AtStr1wPS). Fluorescence images of the protoplasts were taken using a confocal laser scanning microscope. The GFP fluorescence was excited with the argon laser (488 nm) and detected at 515 nm to 520 nm. B, The same protoplast suspension was additionally stained with MitoTracker Orange CMTMRos. The fluorescence was excited with the green helium neon laser (543 nm) and detected at 575 nm to 585 nm. C–J, Arabidopsis protoplasts were transiently transformed with *AtStr1* and *AtStr2* constructs with and without the targeting peptide sequences (AtStr1wPS/AtStr1woPS and AtStr2wPS/AtStr2woPS, respectively). Bright field images shown in C, E, G, and I were made to visualize the protoplast's cell membrane and the chloroplasts. Fluorescence images of the protoplasts shown in D, F, H, and J were taken using an Axioskop microscope with filter sets optimal for GFP fluorescence (BP 450–490/LP 520). All scale bars represent 10 μm.

construct of *AtStr1* with the targeting peptide sequence and the GFP-encoding cDNA sequence at the 5′ end (AtStr1wPS/pGFP-C) resulted in a fluorescence image identical to the transformed pGFP-C vector alone (data not shown). This indicates that the N-terminal targeting peptide is recognized by the import machinery of the mitochondria.

Table I. *Overview of the GFP fusion clones produced*

The name of the fusion construct, the length of the PCR amplified DNA fragment, the primer pairs designed with the respective restriction sites, and the respective vector used for the fusions are listed. More information on the respective members of the multiprotein family is available at the Web site http://arabidopsis.org/info/genefamily/STR_genefamily.html.

Protein Name	Base No.	Primer Pairs	Restriction Site	Fusion Vector
AtStr1woPS	963	P194 5′-cca tgg ctt cta ctg gag ttg a-3′	*Nco*I	pGFP-N
		P195 5′-cca gat ctt gaa gaa gat tca ac-3′	*Bgl*II	pGFP-C
AtStr1wPS	600	P192 5′-cca tgg cct cga ccc ttt tct-3′	*Nco*I	pGFP-N
		P193 5′-gga tcc cca tct tgg tag acc t-3′	*Bam*HI	
AtStr2woPS	954	P153 5′-cca tgg ctt ctt ctg gat ctg a-3′	*Nco*I	pGFP-N
		P154 5′-gga tcc tga aga aga acc cac t-3′	*Bam*HI	pGFP-C
AtStr2wPS	1,098	P155 5′-cca tgg cac gag gag aat ctg-3′	*Nco*I	pGFP-N
		P154 5′-gga tcc tga aga aga acc cac t-3′	*Bam*HI	
AtStr14	711	P138 5′-cca tgg ctt cac tta ctt caa-3′	*Nco*I	pGFP-N
		P189 5′-cag atc tgt ctt ctt caa ttg ttt c-3′	*Bgl*II	
AtStr15	546	P132 5′-cca tgg aaa cca ctg ctt tta ac-3′	*Nco*I	pGPF-N
		P150 5′-aga tct ctc ttc tac cgg cag c-3′	*Bgl*II	pGFP-C
AtStr16	360	P134 5′-cca tgg acg agg aga gca gag t-3′	*Nco*I	pGFP-N
		P151 5′-aga tct ttg aag aag aag gag acg-3′	*Bgl*II	
AtStr18	408	P136 5′-cca tgg ctc aat caa tct cct cc-3′	*Nco*I	pGFP-N
		P152 5′-aga tct att agc aga tgg ctc ctc-3′	*Bgl*II	pGFP-C

AtStr2 protein was described to be cytoplasmic (Hatzfeld and Saito, 2000; Nakamura et al., 2000). However, the 5′ end of the *AtStr2* sequence was possibly not correctly determined, since the EST clone ATTS6033 obtained from the Arabidopsis Biological Resource Center, Ohio State University, contained a putative targeting peptide of 48 amino acids (Table II; Papenbrock and Schmidt, 2000b). Therefore protoplasts were transformed with the respective constructs including or excluding the 5′ extension (AtStr2wPS/pGFP-N, AtStr2wPS/pGFP-C, and AtStr2woPS/pGFP-N). All AtStr2 fusion proteins remained in the cytoplasm. Obviously, the additional DNA at the 5′ end did not encode a putative targeting peptide (Fig. 1, G–J; AtStr2wPS/pGFP-C localization data not shown).

To demonstrate the reliability of localization studies using GFP fusion proteins, methods based on antibody specificity were applied. Mitochondria were purified from Arabidopsis cell cultures, chloroplasts were enriched from green Arabidopsis plants, and total protein extracts were prepared from green Arabidopsis plants. In the western-blot analysis, a protein of about 35 kD was detected in the mitochondrial fraction, corresponding to the predicted size of the mature AtStr1 protein (35.6 kD; Fig. 2A). In total extracts, a protein of about 43 kD was found close to the

Table II. *Localization of sulfurtransferases*

The protein name, gene identification, and the number of amino acids for six selected Str are summarized. PSORT and TargetP were used for the localization prediction, and SignalP V2.0 was used for the cleavage site prediction (http://www.expasy.ch/tools). Numbers in brackets give the certainty of prediction in PSORT; for the TargetP program, the respective probabilities are given; only the two highest scores of both programs are given. The results of the experiments done are summarized. aa, amino acids; Chl/c, chloroplast; Cyt, cytoplasm; exp., experimental; ID, identification; Mit/m, mitochondrial; n.d., not determined; SP, secretory pathway; TP, targeting peptide.

Name	Gene ID	No. aa	Localization Prediction		Exp.
		TP/total	PSORT	TargetP	
AtStr1	At1g79230	58/379	Mit matrix space (0.814)	cTP - 0.666	Mit
			microbody (peroxisome) (0.579)	mTP - 0.319	
AtStr2	At1g16460	48/366	Chl stroma (0.607)	cTP - 0.233	Cyt
			Cyt (0.450)	SP - 0.165	
AtStr14	At4g27700	34/237	Chl stroma (0.950)	cTP - 0.816	Chl
			Chl thylakoid membrane (0.800)	mTP - 0.258	
AtStr15	At4g35770	63/182	Chl stroma (0.837)	cTP - 0.822	Chl
			Mit matrix space (0.598)	mTP - 0.067	
AtStr16	At5g66040	79[a]/120	Cyt (0.450)	SP - 0.136	Chl
			Mit matrix space (0.360)	mTP - 0.108	
AtStr17	At2g17850	28[a]/150	Nucleus (0.760)	SP - 0.136	n.d.
			microbody (peroxisome) (0.364)	mTP - 0.074	
AtStr18	At5g66170	10[a]/136	Chl stroma (0.889)	cTP - 0.237	Cyt
			Chl thylakoid membrane (0.555)	SP - 0.120	

[a]The prediction probability of the targeting peptide is low.

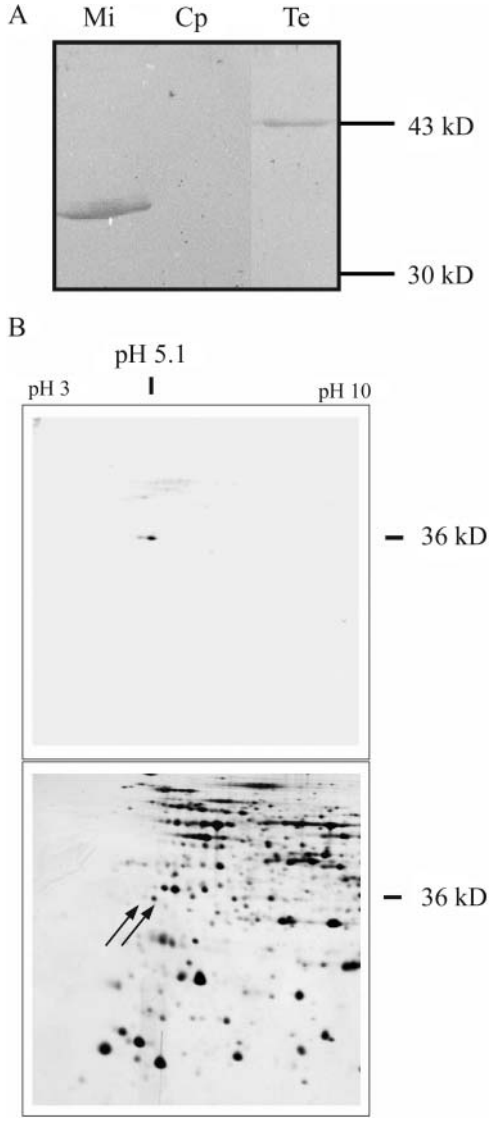

Figure 2. Protein gel electrophoresis and subsequent western-blot analysis of total and organellar extracts. A, Mitochondria (Mi) were purified from Arabidopsis cell cultures, chloroplasts (Cp) were isolated from green Arabidopsis plants, and total soluble protein extracts (Te) were also obtained from green Arabidopsis plants. The proteins were separated by one-dimensional gel electrophoresis, blotted, and the membranes were incubated with an antibody directed against the AtStr1 protein. B, Mitochondria were purified as described above. Their proteome was separated by two-dimensional gel electrophoresis and analyzed by western-blot analysis as described above (top). The corresponding protein spots marked by arrows were localized on a Coomassie-stained gel that was run in parallel. The spots were cut and the proteins were analyzed by mass spectrometry.

predicted size of the AtStr1 protein including the targeting peptide (41.9 kD).

The proteome of mitochondria purified from Arabidopsis cell cultures was separated by two-dimensional gel electrophoresis (50 μg protein) and was subject to western-blot analysis (Fig. 2B, top). In comparison to the western blot of the one-dimensional gel, the development of the color reaction was prolonged to detect as many cross-reacting proteins as possible without obtaining too much background. Two protein spots, a major and a minor, were identified in the immunoreaction. The molecular mass and the pI of the major spot are in agreement with the predicted values (35.6 kD/pI 5.01) of the mature AtStr1 protein. In parallel, the mitochondrial proteome (1 mg protein) was separated under the same conditions, and the gel was Coomassie-stained. The protein spots corresponding to the proteins recognized by the AtStr1-specific antibody are marked by arrows (Fig. 2B, bottom). In the MALDI/TOF-MS and ESI-MS/MS analysis, both the major and the minor protein spots were identified as AtStr1 proteins. The difference in the molecular mass may be explained by a posttranslational modification, such as a phosphorylation. The nature of the modification is still unknown. The sequence of the N-terminal peptide of the mature AtStr1 could be determined, and the computer-predicted cleavage site was confirmed experimentally. The total length of targeting peptide was calculated to 58 amino acids; the bar marks the cleavage site: MASTL…WARRA_MASTG.

Three Single-Domain AtStrs Are Localized in Chloroplasts and One Is Localized in the Cytoplasm

Group VI of the AtStr family contains five members which have single-domains (Table II). To clarify their function, as many features as possible of each single AtStr should be determined. Intracellular localization of four of the single-domain AtStrs was analyzed. To date, no EST clone of AtStr17 has been isolated (http://www.uni-frankfurt.de/fb15/botanik/mcb/AFGN/papen.htm). RT-PCR using different mRNA-pools and screening of cDNA libraries with sequence specific primers was not successful, indicating that the gene encoding AtStr17 may be a pseudogene.

Nicotiana tabacum leaf cells were transformed with the transient expression system with the fusion constructs AtStr14/pGFP-N and AtStr14/pGFP-C or AtStr18/pGFP-N and AtStr18/pGFP-C using the ballistic method of particle gun bombardment. Transformed tobacco leaf epidermal and guard cells were analyzed by fluorescence microscopy after overnight incubation (Fig. 3). AtStr14 was transported into plastids as seen in the images of the GFP fluorescence in plastids of epidermal and guard cells (Fig. 3, B and C). The bright field image of an epidermal *N. tabacum* cell shows the cell dimensions (Fig. 3A). In pretests, leaves of Arabidopsis were also transformed by particle bombardment and led to the same localization of the Arabidopsis proteins as the heterologous transformation of *N. tabacum* leaves. Controls using a GFP fusion construct containing the transit peptide of Rubisco revealed comparable images, as shown in Figure 3, B and C (data not shown). Figure 3, D and E, show the same guard cell transformed with the AtStr18/pGFP-N construct: GFP fluorescence was detected in the cytoplasm.

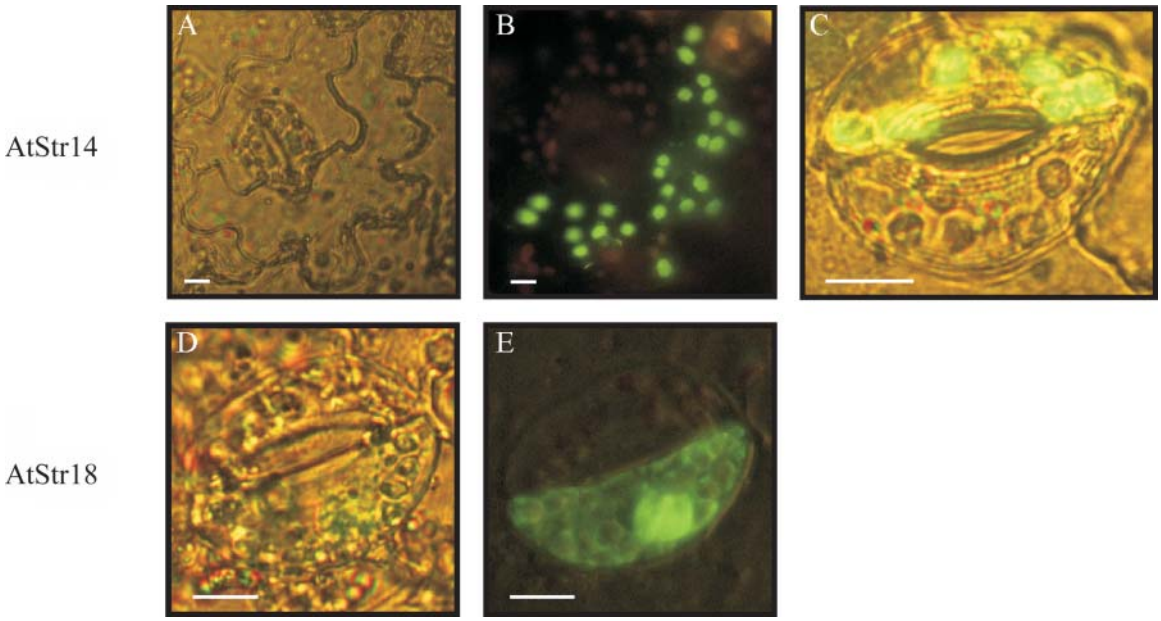

Figure 3. Localization of the single-domain Str AtStr14 and AtStr18 in tobacco leaf epidermal and guard cells. Fusion constructs of AtStr14 and AtStr18 with the GFP encoding sequence were transformed in *N. tabacum* leaf cells by particle gun bombardment and were analyzed by fluorescence microscopy after overnight incubation. A, Bright field image of an epidermal *N. tabacum* cell. B, In the same cell shown in A, the fluorescence of the AtStr14/pGFP-N fusion protein was collected with the band pass filter (BP 450–490) for excitation and with the long pass filter (filter LP 520) for emission. C, Single merged image of a guard cell for AtStr14. D, Bright field image of a guard cell. E, In the same guard cell shown in D, the fluorescence was collected as described in B. All scale bars represent 10 μm.

To examine targeting of four out of five of the single-domain AtStr, fusion constructs of AtStr14, AtStr15, AtStr16, and AtStr18 with pGFP-N or pGFP-C were introduced into Arabidopsis protoplasts, incubated overnight at room temperature, and visualized by fluorescence microscopy (Fig. 4). Bright field images were taken to visualize the protoplast's cell membrane and chloroplasts. AtStr14, AtStr15, and AtStr16 were localized in chloroplasts, whereas AtStr18 remained in the cytoplasm. The choice of the transformation method, either particle bombardment or polyethylene glycol-mediated protoplast transformation, did not affect the localization results as shown by Figures 3 and 4.

The AtStr15 Protein Is Associated with the Thylakoid Membrane

In contrast to AtStr14 and AtStr16, which were evenly distributed in the chloroplasts which is indicative for soluble proteins, the intracellular localization of the AtStr15 protein was unusual (Fig. 4). It was not possible to unambiguously determine whether the protein was outside of the chloroplast, on the chloroplast envelope, or attached to the thylakoid membranes inside the chloroplast. Therefore we investigated its localization in more detail. Protoplasts were transiently transformed with AtStr15/pGFP-N and analyzed with the CLSM (Fig. 5). In Figure 5C, the merged image of GFP fluorescence and chlorophyll autofluorescence of the same protoplast is shown. In Figure 5D, coordinating lines show the localization of AtStr15 (shown on the sidelines) in more detail. A higher magnification of the same protoplast enabled visualization of the thylakoid membranes and indicated an association of AtStr15 with the thylakoid membrane (Fig. 5, E and F). However, the limited resolution of the CLSM and the extensive emission of the GFP fluorescence made a final conclusion with respect to the subcellular localization of AtStr15 difficult.

Transmission electron immunomicroscopy was used to investigate the subcellular localization further. Protoplasts were transformed with AtStr15/pGFP-N using a transient expression system and then incubated with antibodies directed against GFP, and the secondary antibody was labeled with gold particles. The transmission images show an association of AtStr15 protein with the thylakoid membranes and to a smaller extent localization in the stroma of the chloroplasts (Fig. 6).

The statistical analysis of the density of gold labeling in the chloroplasts indicates an effective transformation. In 43 mitochondria, only a total of 3 gold particles were found; in the profiles of the plasma membrane from 10 protoplasts just 4 gold particles were detected. In an area of 152 μm^{-2} of cytoplasm, 38 gold particles were counted. In 27 chloroplasts, with an area of 144 μm^{-2}, 234 gold particles were found. More than 74% of the gold label in chloroplast was associated with the thylakoid membranes, the remaining in stroma (Table III). As controls for the specificity of the

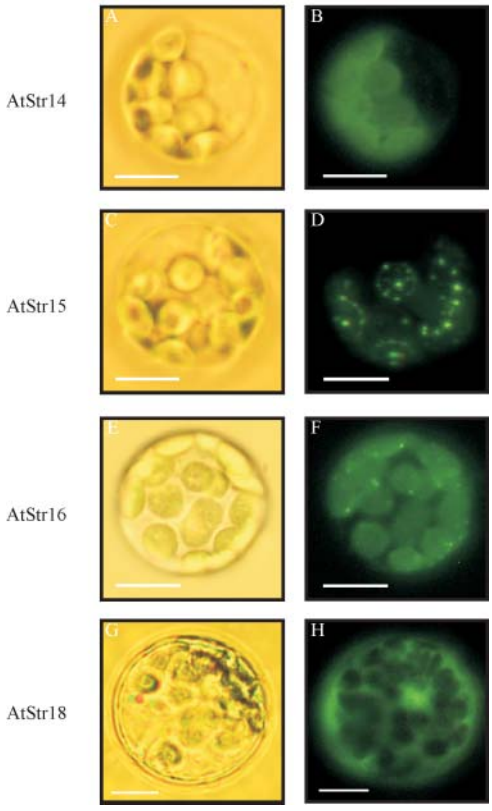

Figure 4. Targeting analysis of all members of the AtStr group VI visualized by fluorescence microscopy. The fusion constructs of AtStr14, AtStr15, AtStr16, and AtStr18 with pGFP-N were introduced into Arabidopsis protoplasts. The protoplasts were incubated overnight at room temperature and then analyzed with an Axioskop microscope with filter sets optimal for GFP fluorescence (BP 450–490/LP 520). Bright field images (A, C, E, and G) were made to visualize the protoplast's cell membrane and chloroplasts. Fluorescence images of the same protoplasts are shown in B, D, F, and H.

attachment, sections were incubated either in the absence of the GFP-specific antibody or with preimmune serum. Less than 1 gold particle per 10 μm^{-2} was seen in these control sections. Only a few areas around some vacuoles displayed 2 or 3 gold particles above this background. However, this compartment is known as having relatively high unspecific affinity.

Computer-Based Prediction of Protein Localization Compared with Experimental Results

Several computer programs using different algorithms for the prediction of the intracellular localization of proteins were applied. The results of the prediction by computer programs are summarized in Table II. For three out of six proteins, the localization predictions were in agreement with the experimental results (AtStr1, AtStr14, and AtStr15). For these proteins the probabilities given by both programs PSORT and TargetP were very high. However, results in TargetP for AtStr1 suggested a dual-targeting into mitochondria and chloroplasts. The prediction probabilities for the other three proteins gave lower values, except for a chloroplast stroma localization of AtStr18 in PSORT. In the case of these lower certainties for the prediction, the experimental data gave completely different results.

DISCUSSION

The Targeting Peptide of the Nuclear Encoded AtStr1 Protein Is Cleaved after Being Imported into Mitochondria

All Str proteins identified in Arabidopsis are nuclear-encoded proteins (Bauer and Papenbrock, 2002). Most of them were predicted to contain N-terminal do-

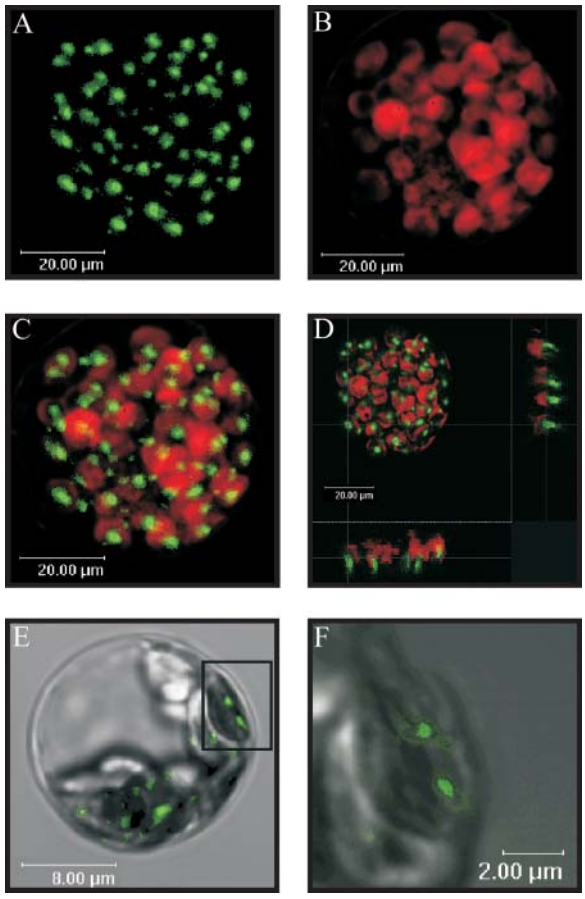

Figure 5. Detailed analysis of the subcellular localization of AtStr15. Arabidopsis protoplasts were transformed with the AtStr15/pGFP-N fusion construct. All images (A–F) were made with the True Confocal Scanner. GFP fluorescence was excited with an argon laser (488 nm) and detected at 515 nm to 520 nm. Chlorophyll autofluorescence (red) was detected simultaneously at 650 nm to 670 nm. A, GFP fluorescence in a transformed protoplast. B, chlorophyll fluorescence of the same protoplast as in A. C, Merged image of A and B. D, This figure represents the image shown in C having coordinating lines to show the localization of AtStr15 (shown on the sidelines). E, GFP fluorescence of a single chloroplast merged with the respective bright field image. F, Enlarged image of the inset of Figure E. The sizes of the scale bars are given directly in the images.

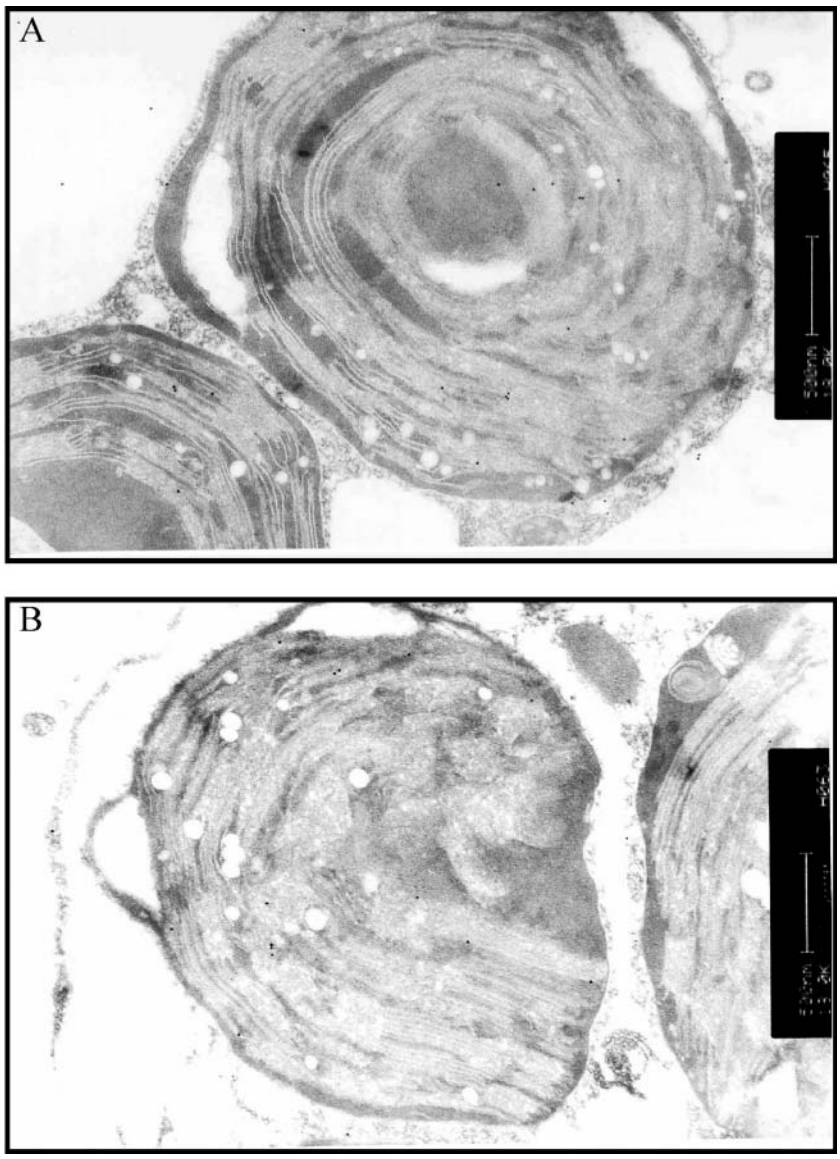

Figure 6. Immunogold localization of GFP fusion protein in transiently transformed protoplasts by transmission electron microscopy. A, Chloroplast with numerous (>12) gold particles (i.e. GFP immunoreactivity) close to another chloroplast with and to a mitochondrion (below) without immunogold label. B, Chloroplast at the left with about 12 gold particles at the thylakoid membrane. The mitochondrion at the right has no label. The chloroplast at the right contains only one label at the thylakoid membrane. The plasma membrane of the protoplast has one gold label. The scale bars represent 500 nm.

mains potentially specifying intracellular targeting. The AtStr1 protein was shown previously to be localized in mitochondria by western-blot analysis (Nakamura et al., 2000; Papenbrock and Schmidt, 2000a) and GFP fusions (Hatzfeld and Saito, 2000; Nakamura et al., 2000). However, for the AtStr1 full-length fusion protein, a dual-targeting was observed and also shorter versions of AtStr1 fused to GFP were found to target not only mitochondria, but also chloroplasts. On the basis of further localization experiments, the authors concluded that the dual-targeting done with different GFP constructs did not reflect the actual subcellular distribution of AtStr1 in the plant cell (Nakamura et al., 2000). Very short fusion constructs might result in artifacts with respect to the intracellular localization (personal communication, Dr. R. Hänsch, Braunschweig). In our hands, the fusion of the N-terminal extension of AtStr1 alone to GFP led to nonreproducible results, mainly indicating a cytoplasmic localization (data not shown). Therefore only the full-length proteins including their N-terminal or C-terminal extensions were used in this study. All AtStr sequences were ligated into both vectors pGFP-N and pGFP-C and were transiently transformed. The GFP fluorescence of fusions with the pGFP-C vector always resulted in the same image as the pGFP-C and pGFP-N vector without any additional insert (data not shown). This fact indicates that none of the proteins investigated contained C-terminal targeting peptides for other compartments, such as the peroxisomes or the endoplasmatic reticulum (Emanuelsson and von Heijne, 2001).

The western-blot analyses of organelle and total protein extracts showed a mitochondrial localization of the mature AtStr1 protein. To identify the correct cleavage site, mitochondria were isolated from sus-

Table III. *Summary of the data of the immunolabeling studies*

Data were collected from 20 fields analyzed in 5 ultrathin sections from 2 blocks of transiently transformed protoplasts according to Griffiths (1993). In sections incubated either in the absence of antibody or with preimmune serum, less than 1 gold particle per 10 μm^{-2} was seen. The means ± SDs are given. gp, gold particles.

Organelle	Density of Immunogold Label (gp 10 μm^{-2})
Mitochondria	Below detection limit
Plasma membrane	Below detection limit
Cytoplasm	3.6 ± 2.1
Chloroplasts[a]	18.5 ± 6.0

[a]More than 74% of the label is associated with the thylakoid membranes.

pension cell cultures, the mitochondrial proteome was separated by two-dimensional gel electrophoresis, and AtStr1 was detected by using a monospecific antibody against the protein. The determined size and pI corresponded with the computer prediction. The sequence of the mature protein's N terminus, and therefore the cleavage site, matched the predictions. In this particular case, all prerequisites for a successful application of this method were fulfilled. For a widespread use there are limitations, such as the availability of monospecific antibodies. In addition, the isolation of pure organelles from cell cultures is a compromise since the correct localization of proteins might be affected by the intactness of the whole plant organism. However, the isolation of mitochondria (Hausmann et al., 2003) or other organelles from tissue of intact plants (Fukao et al., 2002) can be very difficult. Altogether the approach is rather laborious. Nevertheless for some proteins the method is successful.

Recently a high throughput analysis of the Arabidopsis mitochondrial proteome derived by liquid chromatography-tandem mass spectrometry was reported (Heazlewood et al., 2004). The AtStr1 protein and a second AtStr protein, AtStr3, which has not yet been characterized in detail (Bauer and Papenbrock, 2002) were identified as mitochondrial proteins by this approach. However, a number of false-positives, for example several well-known plastidic proteins (e.g. At5g13630, At5g43780), were also found in the mitochondrial fraction, which reduces the reliability of this approach. Therefore the individual analysis of proteins with respect to the intracellular localization is still needed.

The Single-Domain AtStr Are Not Localized in Mitochondria

The transient transformation of Arabidopsis protoplasts using GFP fusion constructs was successfully established in our laboratory as described above. To confirm the translocation results obtained by this method, intact cells of *N. tabacum* and Arabidopsis leaves, respectively, were additionally transiently transformed by particle bombardment with two single-domain AtStrs. It was reported that the translocation of proteins might be species-dependent. A homologous system was recommended, at least for import experiments of dual-targeting proteins (Lister et al., 2001). In our experiments, no difference could be observed between the use of tobacco and Arabidopsis leaves with respect to the yield of transformed cells and with respect to the intracellular localization of the Arabidopsis proteins. For practical reasons, in most of the particle bombardment experiments tobacco leaves were transformed. The plastids of epidermal cells in higher plants contain almost undetectable amounts of pigments. Therefore the plastids are not visible in the bright field image (Fig. 3A), but the GFP fluorescence of the AtStr14 fusion protein indicates their presence and abundance (Fig. 3B). AtStr14 and AtStr16 are soluble proteins equally distributed in the chloroplasts, similarly to the distribution of the soluble Rubisco protein, whose transit peptide was initially used in GFP control constructs (data not shown).

It has been speculated that Str proteins are involved in iron-sulfur cluster biosynthesis in mitochondria and plastids as a donor of reduced sulfur (Bonomi et al., 1977; Cerletti, 1986). The two-domain AtStr proteins, AtStr1 and AtStr2, are localized in the mitochondrion and the cytoplasm, respectively (Hatzfeld and Saito, 2000; Nakamura et al., 2000; Papenbrock and Schmidt, 2000a, this work). Both proteins belong to the group of 3-mercaptopyruvate AtStrs. Therefore the localization of three AtStr proteins in the plastids provides the basis for new experiments with respect to iron-sulfur cluster biosynthesis. For two out of three plastid-localized single-domain AtStrs, thiosulfate Str activity could already be shown in vitro (Bauer and Papenbrock, 2002). Recently, a plastidic NifS-like Cys desulfhydrase was also suggested to be involved in iron-sulfur cluster biosynthesis (Leon et al., 2002). However, several proteins, both NifS-like and Str, might be involved in providing the reduced sulfur.

The Subcellular Localization of AtStr15

The AtStr15 protein localization data was unusual: it might be associated with the chloroplast membrane or localized inside the chloroplasts (Fig. 4D). Recently, the intracellular localization of a *N. tabacum* protein, Ntdin, with 56.8% sequence identity to AtStr15 on the amino acid level was exclusively found in chloroplasts (Yang et al., 2003). The Ntdin protein was evenly distributed in this organelle. The Ntdin and the AtStr15 protein possess high sequence homologies to the Din1 protein from *Raphanus sativus*, the first chloroplast protein detected that was negatively regulated by light. The Din1 protein was shown to be senescence-associated and has sequence similarity to sulfide dehydrogenase or other small stress proteins (Shimada et al., 1998). However, both proteins could be paralogs or orthologs and do not necessarily need to have the same function in the plant cell. Different

subcellular localizations of very similar proteins may also occur.

The resolution in cell images visualized by fluorescence microscopy is sufficient for the localization of soluble organellar proteins and can be merged with the autofluorescence images. However, the investigation of subcellular detail can be drastically improved by the ability to show single nm sections of the cell by CLSM, compared to the fluorescence microscope in which the fluorescence of the whole protoplast is collected. The highly magnified CLSM images of cells transformed with AtStr15 (Fig. 5, E and F) were the grounds for assuming an association with the thylakoid membrane. The images of immunogold labeling by transmission electron microscopy and their statistical evaluation support a preferential association of the AtStr15 molecules to the thylakoid membranes inside the chloroplast. The AtStr15 C terminus contains a hydrophobic region of about 20 amino acids, which is predicted to be transmembrane or membrane-associated (Transmembrane Hidden Markov Model; http://www.expasy.ch/tools). Therefore we assume that the protein is attached to the thylakoid membrane by the C terminus. Studies on a peroxiredoxin protein indicated that the decameric form was attached to the thylakoid membrane, and this depended on the physiological status of the cell (Konig et al., 2002). Future experiments need to be done to explain the function of the membrane-associated AtStr15 protein. The substrate for this putative AtStr might involve another protein which could be activated or deactivated by the transfer of a reduced sulfur.

Computer-Based Prediction of Protein Localization Is Not Reliable

The computer-based localization prediction for all AtStrs gave putative localizations in the cytoplasm, chloroplast stroma and thylakoid membrane, mitochondrion, peroxisome, and nucleus (Table II). Our experimental approach revealed that the intracellular computer localization predictions were correct for only three out of six proteins. In a study by Millar et al. (2001), the computer prediction of intracellular localization has been shown to be error prone for individual sequences. Out of a set of 91 proteins detected in purified Arabidopsis mitochondria, only 50 to 55 were predicted to be mitochondrial upon analysis with prediction programs. In a high throughput analysis of the Arabidopsis mitochondrial proteome (Heazlewood et al., 2004), approximately one-half of the experimental set was predicted to be mitochondrial by targeting prediction programs.

The prediction programs use different algorithms. PSORT is based on an expert system with a knowledge-base and is a collection of ''if-then''-type rules (Nakai and Kanehisa, 1992). TargetP is a neural-network-based tool for large-scale intracellular location prediction of proteins. Using N-terminal sequence information only, it discriminates between proteins destined for the mitochondrion, the chloroplast, the secretory pathway, and other localizations with a calculated success rate of 85% (plant) and 90% (nonplant) redundancy-reduced test sets (Emanuelsson et al., 2000). The correctness of the cleavage site prediction was determined to 40% to 50% for chloroplast transit peptides and mitochondrial presequences, and to above 70% for secretory signal peptides. The algorithms for the localization prediction of plant proteins need to be improved. The occurrence of an additional compartment, the plastid, evolved from an endosymbiotic event and surrounded by a double lipid bilayer, causes many dual-targeting predictions. As more proteins are localized by experimental methods, more targeting peptides will be available as models for the development of new algorithms.

CONCLUSIONS

The members of the multiprotein family of Arabidopsis Str investigated are localized in the cytoplasm, in the mitochondrion, and in plastids. The mitochondrial localization of AtStr1 was shown by western-blot analysis and transient expression of GFP fusion constructs. The transient transformation of either leaf cells or protoplasts with GFP fusion constructs gave similar results. Three of the single-domain AtStr are translocated to plastids, and AtStr15 is closely associated with the thylakoid membrane. The prediction of localization using several computer programs based on different algorithms is correct only to about 50%. Therefore biochemical analysis of the intracellular localization of individual proteins is still required in the age of high-throughput methods and bioinformatics.

MATERIALS AND METHODS

Plant Material

Arabidopsis Heynh. (ecotype C24) and *Nicotiana tabacum* L. (cv Samsun NN) plants were grown on soil in the greenhouse in a 16 h light/8 h dark cycle at a temperature of 23°C/21°C. When necessary, additional light was switched on for 16 h per day to obtain a constant quantum fluence rate of 300 μmol m^{-2} s^{-1} (sodium vapor lamps, SON-T Agro 400, Philips, Eindhoven, The Netherlands). Arabidopsis (ecotype C24) suspension cultures were established and grown as described by May and Leaver (1993).

DNA Cloning Techniques

The origins of templates and conditions for the amplification of cDNAs encoding AtStr1 (At1g79230), AtStr2 (At1g16460), AtStr15 (At4g35770), AtStr16 (At5g66040), and AtStr18 (At5g66170) have been described previously (Papenbrock and Schmidt, 2000a, 2000b; Bauer and Papenbrock, 2002). For the amplification of a cDNA sequence encoding AtStr14 (At4g27700), the full length EST clone RAFL05-17-G02 was obtained from RIKEN BioResource Center, Tsukuba, Japan. All primer pairs used for the construction of fusion clones with the GFP are listed in Table I.

The PCR contained 0.2 mM dNTPs (Roth, Karlsruhe, Germany), 0.4 μM of each primer (MWG, Ebersberg, Germany), 1 mM $MgCl_2$ (final concentration, respectively), 0.75 μL RedTaq DNA-Polymerase (Sigma, Taufkirchen, Germany), and about 1 μg template DNA in a final volume of 50 μL. Before starting the first PCR cycle, the DNA was denatured for 180 s at 94°C, fol-

lowed by 28 PCR cycles of 45 s at 94°C, 45 s at 55°C, and 45 s at 72°C each. The process was finished with an elongation phase of 420 s at 72°C. The amplified PCR fragments were ligated into pBSK-based enhanced GFP containing vectors to obtain either GFP fusions with the 5′ end of the GFP coding sequence (pGFP-N) or with the 3′ end (pGFP-C) and were introduced into the *Escherichia coli* strain XL1-blue. The gene-cassettes were driven by the CaMV-35S promoter with a double enhancer and the polyA-tail from CaMV-35S. Clones were sequenced for conformation of the insert using specific primers GFPforward 5′-CTGGAGTTCGTGACCGCCGCCGG-3′ or GFPreverse 5′-GCTTGCCGTAGGTGGCATCGCCCT-3′ (MWG Biotech, Ebersberg, Germany). The expressed Str proteins were either fused with the N terminus of the GFP (pGFP-N) or with the C terminus of the GFP (pGFP-C).

Transient Expression of GFP Fusion Constructs in *N. tabacum* Leaves

Plasmid DNA from the constructs described above was column-purified (Plasmid Midi Kit, Qiagen, Hilden, Germany). Gold particles (1.0 μm gold microcarrier, Bio-Rad Laboratories GmbH, Munich) were covered with plasmid DNA as follows (protocol for 6 repetitions): 3 mg gold was washed in pure 70% ethanol, centrifuged for 1 min at 1,925*g* with braking. The gold pellet was resuspended in 50 μL H_2O and again centrifuged at 47*g* without braking. The pellet was resuspended in 50 μL 50% glycerol by mixing and ultrasonification for 10 s. After adding 7 μg plasmid DNA dissolved in 7 μL H_2O and incubation for 5 min on ice, 50 μL 2.5 M $CaCl_2$ and 20 μL cold 1 M spermidine were added. The suspension was centrifuged for 15 s at 47*g* and the pellet was resuspended in 100% ethanol by mixing and ultrasonification. For the bombardment, 5 μL of the DNA-covered gold particles were distributed on a macrocarrier/flying disc (Bio-Rad). The rupture discs (Bio-Rad) used could withstand 900 pounds per square inch. Pieces (4 × 4 cm) of fully expanded *N. tabacum* leaves were cut from 4-week-old plants by avoiding the middle rib. The leaf pieces were placed upside down on moistened filter paper in petri dishes (9 cm diameter). The particle delivery system was used according to the manufacturer's instructions (Bio-Rad). The treated leaf pieces were incubated for about 16 h at room temperature. Then the epidermis of the tobacco leaves was removed and placed in 0.3 M sorbitol on a glass slide for microscopic analysis.

Transient Expression of GFP Fusion Constructs in Arabidopsis Protoplasts

The younger rosette leaves of 3-week-old Arabidopsis plants were used for the preparation of protoplasts according to Damm et al. (1989), Sheen (1995), and Abel and Theologis (1998) with some modifications. About 40 leaves were cut in 1 mm strips with sharp razor blades and put in 6 mL of medium I (1% [w/v] cellulase Onozuka R-10, 0.25% [w/v] macerozyme R-10 [Yakult Honsha, Tokyo], 0.4 M mannitol, 20 mM KCl, 20 mM MES/KOH, pH 5.7, 10 mM $CaCl_2$, 5 mM β-mercaptoethanol, and 0.1% [w/v] bovine serum albumine). After application of a vacuum for 15 min, the leaves were incubated on a shaker (40 rpm) for 60 min at room temperature. The suspension was filtered through a 75 μm-pore nylon net, distributed on 4 2 mL-tubes, and centrifuged for 2 min at 95*g* and 4°C. The pellets were washed twice with 500 μL of medium II (154 mM NaCl, 125 mM $CaCl_2$, 5 mM KCl, and 2 mM MES/KOH, pH 5.7) and finally incubated for 30 min on ice in medium II. After centrifugation for 2 min at 95*g* and 4°C, the pellets were carefully resuspended in 150 μL of medium III (0.4 M mannitol, 15 mM $MgCl_2$, and 4 mM MES/KOH, pH 5.7). For the transformation, 100 μL of the protoplast suspension was mixed carefully with 15 μg column-purified plasmid DNA and 110 μL medium IV (4 g polyethylene glycol 4,000, 3 mL H_2O, 2.5 mL 0.8 M mannitol, and 1 mL 1 M $CaCl_2$), and incubated for 30 min at 23°C. To remove the polyethylene glycol, the solution was washed with 1 mL of medium II and centrifuged for 2 min at 95*g* and 4°C. The pellet was resuspended in 50 μL of medium II and incubated overnight at room temperature.

In some experiments MitoTracker Orange CMTMRos (Molecular Probes, Eugene, OR) was used to stain mitochondria. The dye was dissolved in dimethyl sulfoxide to 1 mM and was incubated in a final concentration of 0.5 μM with the protoplast suspension for 15 min.

Microscopic Analysis

The transiently transformed cells and protoplasts were analyzed with an Axioskop microscope (Carl Zeiss, Jena, Germany). The GFP fluorescence was collected with the band pass filter (BP 450–490) for excitation and with the long pass filter (LP 520) for emission. The generation of transmission micrographs for visualization of nonfluorescent protoplast structures was achieved using the manufacturer's filter settings. Confocal imaging of transformed protoplasts and stained mitochondria was performed with the True Confocal Scanner (Leica, TCS SP2, Solms, Germany). Specimens were examined using Leica 20x and 63x water immersion objectives. GFP fluorescence was excited with the argon laser (488 nm) and detected at 515 nm to 520 nm. MitoTracker Orange CMTMRos was excited with the green helium neon laser (543 nm) and detected at 575 nm to 585 nm. Far-red autofluorescence of chlorophyll was detected at 650 nm to 670 nm. All images were edited with Corel Photo Paint 10.

Localization Studies by Immunogold Electron Microscopy

The suspension of protoplasts was centrifuged at 375*g* in an Eppendorf microtube; the sediment was layered with 10 uL 1.5% gelatin in medium II and was then cooled on ice. After solidification of the gelatin, the samples were covered with 1 mL of fixative, consisting of 4% (w/v) freshly depolymerized paraformaldehyde prepared in medium II and containing 0.5% (w/v) glutaraldehyde. After fixation for 30 min at 4°C, the samples were washed with medium II, dehydrated at low temperature with graded alcohols, and embedded in LR-Gold as described previously (Sierralta, 2001). From the embedded tissues, ultrathin sections (70 nm thickness) were cut with a Reichert-Jung ultramicrotome; the sections were collected on Formvar-coated 200 mesh gold grids and immediately incubated as described (Sierralta et al., 1995). Briefly, after quenching and blocking, the ultrathin sections were incubated for 2 h at room temperature with rabbit anti-GFP (Molecular Probes, Eugene, OR) and thoroughly washed. The bound IgGs were tagged with goat anti-rabbit IgG labeled with 15 nm gold particles (British BioCell, Cardiff, UK). Finally, the sections were lightly stained with 5% aqueous uranyl acetate and Reynolds lead citrate. Immunolabeling controls included omission of the primary antibody or incubation of the sections with serum from a nonimmunized rabbit. Sections were viewed with a Philips CM100 electron microscope at 80 kV, photographed on Kodak 4489 EM film, and printed on Agfa photographic paper. The digital images are from scans of the photomicrographs. A statistical analysis of the immunolabeling results was done according to established criteria (Griffiths, 1993). Data were collected from 20 fields analyzed in 5 sections from 2 blocks of protoplasts from transiently transformed leaves. The primary magnification used was 18,000x.

Organelle Isolation, SDS-PAGE, and Western Blotting

Mitochondria were isolated from Arabidopsis suspension cultures as described by Kruft et al. (2001). Chloroplasts were isolated from 4-week-old Arabidopsis plants according to Jensen and Bassham (1966). Total protein extracts from Arabidopsis plants were obtained as described previously (Papenbrock and Schmidt, 2000b). Aliquots of approximately 10 μg protein determined following the method of Stoscheck (1990) were analyzed by one-dimensional SDS-PAGE (Laemmli, 1970). The mitochondrial proteome was separated by two-dimensional gel electrophoresis (50 μg protein, IEF range pH 3–10; Kruft et al., 2001). The resulting gels were blotted onto nitrocellulose membranes (Sambrook et al., 1989). For immunodetection, a monospecific antibody directed against the recombinant AtStr1 protein was used (Papenbrock and Schmidt, 2000a). The protein spots corresponding to the immunostained proteins were localized on a Coomassie-stained (Neuhoff et al., 1985) two-dimensional gel loaded with 1 mg mitochondrial protein and analyzed by mass spectrometry.

Miscellaneous

The analyses of DNA and amino acid sequences were performed with the programs EditSeq and MapDraw in DNASTAR (Madison, WI). For the computer-based prediction of the protein localization, different programs were applied (mainly PSORT, SignalP V2.0, TargetP, and further programs in http://www.expasy.ch/tools). After the transient transformation methods had been established, the transformations were performed with each clone at least five times, resulting always in the same intracellular localization.

ACKNOWLEDGMENTS

We thank P. von Trzebiatowski for her excellent technical assistance. We thank Prof. H.P. Braun and H. Eubel, Hannover, Germany, for carrying out the two-dimensional gel electrophoresis and the western blot. We appreciate the mass spectrometry analysis of Str1 done by Dr. C. Lemaitre-Guillier and Prof. A. Van Dorsselaer, Strasbourg, France. We are grateful to A. Wachter and Prof. T. Rausch (Heidelberg) for the generous donation of GFP control constructs for mitochondrial, peroxisomal, and plastidal localization initially used. Many thanks to Dr. R. Hänsch (Braunschweig, Germany) for his initial help in particle bombardment experiments. In our laboratory, particle bombardment experiments were established by M. Brusch. Prof. Dr. W.D. Sierralta visited Hannover in the frame of the AleChile Academic Exchange Program supported by DAAD and Conicyt (project no. 2001/061). We thank Dr. M. Hawkesford, Rothamsted Research, United Kingdom, for correcting the English language of the manuscript.

Received January 31, 2004; returned for revision March 16, 2004; accepted March 16, 2004.

LITERATURE CITED

Abel S, Theologis A (1998) Transient gene expression in protoplasts of *Arabidopsis thaliana.* Methods Mol Biol **82:** 209–217

Bauer M, Papenbrock J (2002) Identification and characterization of single-domain thiosulfate sulfurtransferases from *Arabidopsis thaliana.* FEBS Lett **532:** 427–431

Bonomi F, Pagani S, Cerletti P, Cannella C (1977) Rhodanese-mediated sulfur transfer to succinate dehydrogenase. Eur J Biochem **72:** 17–24

Bordo D, Bork P (2002) The rhodanese/Cdc25 phosphatase superfamily. Sequence-structure-function relations. EMBO Rep **3:** 741–746

Cerletti P (1986) Seeking a better job for an under-employed enzyme: rhodanese. Trends Biochem Sci **11:** 369–372

Damm B, Schmidt R, Willmitzer L (1989) Efficient transformation of *Arabidopsis thaliana* using direct gene transfer to protoplasts. Mol Gen Genet **217:** 6–12

Donadio S, Shafiee A, Hutchinson R (1990) Disruption of a rhodanese like gene results in cysteine auxotrophy in *Saccharopolyspora erythraea.* J Bacteriol **172:** 350–360

Emanuelsson O, Nielsen H, Brunak S, von Heijne G (2000) Predicting subcellular localization of proteins based on their N-terminal amino acid sequence. J Mol Biol **300:** 1005–1016

Emanuelsson O, von Heijne G (2001) Prediction of organellar targeting signals. Biochim Biophys Acta **1541:** 114–119

Fukao Y, Hayashi M, Nishimura M (2002) Proteomic analysis of leaf peroxisomal proteins in greening cotyledons of *Arabidopsis thaliana.* Plant Cell Physiol **43:** 689–696

Griffiths G (1993) Quantitative aspects of immunocytochemistry. *In* G Griffiths, ed, Fine Structure Immunocytochemistry. Springer Verlag, Berlin, pp 371–445

Hatzfeld Y, Saito K (2000) Evidence for the existence of rhodanese (thiosulfate:cyanide sulfurtransferase) in plants: preliminary characterization of two rhodanese cDNAs from *Arabidopsis thaliana.* FEBS Lett **470:** 147–150

Hausmann N, Werhahn W, Huchzermeyer B, Braun HP, Papenbrock J (2003) How to document the purity of mitochondria prepared from green tissue of tobacco, pea and *Arabidopsis thaliana.* Phyton **43:** 215–229

Heazlewood JL, Tonti-Filippini JS, Gout AM, Day DA, Whelan J, Millar AH (2004) Experimental analysis of the *Arabidopsis* mitochondrial proteome highlights signaling and regulatory components, provides assessment of targeting prediction programs, and indicates plant-specific mitochondrial proteins. Plant Cell **16:** 241–256

Jensen RG, Bassham JA (1966) Photosynthesis by isolated chloroplasts. Proc Natl Acad Sci USA **56:** 1095–1101

Konig J, Baier M, Horling F, Kahmann U, Harris G, Schurmann P, Dietz KJ (2002) The plant-specific function of 2-Cys peroxiredoxin-mediated detoxification of peroxides in the redox-hierarchy of photosynthetic electron flux. Proc Natl Acad Sci USA **99:** 5738–5743

Kruft V, Eubel H, Jänsch L, Werhahn W, Braun HP (2001) Proteomic approach to identify novel mitochondrial proteins in *Arabidopsis thaliana.* Plant Physiol **127:** 1694–1710

Laemmli UK (1970) Cleavage of structural proteins during the assembly of the head of bacteriophage T4. Nature **227:** 680–685

Laudenbach DE, Ehrhardt D, Green L, Grossmann A (1991) Isolation and characterization of a sulfur-regulated gene encoding a periplasmically localized protein with sequence similarity to rhodanese. J Bacteriol **173:** 2751–2760

Leon S, Touraine B, Briat JF, Lobreaux S (2002) The AtNFS2 gene from *Arabidopsis thaliana* encodes a NifS-like plastidial cysteine desulphurase. Biochem J **366:** 557–564

Lister R, Chew O, Rudhe C, Lee MN, Whelan J (2001) *Arabidopsis thaliana* ferrochelatase-I and -II are not imported into *Arabidopsis* mitochondria. FEBS Lett **506:** 291–295

May MJ, Leaver C (1993) Oxidative stimulation of glutathione synthesis in *Arabidopsis thaliana* suspension cultures. Plant Physiol **103:** 621–627

Millar AH, Sweetlove LJ, Giege P, Leaver CJ (2001) Analysis of the *Arabidopsis* mitochondrial proteome. Plant Physiol **127:** 1711–1727

Nagahara N, Ito T, Minami M (1999) Mercaptopyruvate sulfurtransferase as a defense against cyanide toxification: molecular properties and mode of detoxification. Histol Histopathol **14:** 1277–1286

Nagahara N, Okazaki T, Nishino T (1995) Cytosolic mercaptopyruvate sulfurtransferase is evolutionary related to mitochondrial rhodanese. J Biol Chem **270:** 16230–16235

Nakai K, Kanehisa M (1992) A knowledge base for predicting protein localization sites in eukaryotic cells. Genomics **14:** 897–911

Nakamura T, Yamaguchi Y, Sano H (2000) Plant mercaptopyruvate sulfurtransferases: molecular cloning, subcellular localization and enzymatic activities. Eur J Biochem **267:** 5621–5630

Neuhoff V, Stamm R, Eibl H (1985) Clear background and highly sensitive protein staining with Coomassie Blue dyes in polyacrylamide gels: a systematic analysis. Electrophoresis **6:** 427–448

Papenbrock J, Schmidt A (2000a) Characterization of a sulfurtransferase from *Arabidopsis thaliana.* Eur J Biochem **267:** 145–154

Papenbrock J, Schmidt A (2000b) Characterization of two sulfurtransferase isozymes from *Arabidopsis thaliana.* Eur J Biochem **267:** 5571–5579

Ray WK, Zeng G, Potters MB, Mansuri AM, Larson TJ (2000) Characterization of a 12-kilodalton rhodanese encoded by *glpE* of *Escherichia coli* and its interaction with thioredoxin. J Bacteriol **182:** 2277–2284

Sambrook J, Fritsch EF, Maniatis T (1989) Molecular Cloning: A Laboratory Manual, Ed 2. Cold Spring Harbor Laboratory Press, Cold Spring Harbor, NY

Sheen J (1995) Methods for mesophyll and bundle sheath cell separation. Methods Cell Biol **49:** 305–314

Shimada Y, Wu GJ, Watanabe A (1998) A protein encoded by *din1,* a dark-inducible and senescence-associated gene of radish, can be imported by isolated chloroplasts and has sequence similarity to sulfide dehydrogenase and other small stress proteins. Plant Cell Physiol **39:** 139–143

Sierralta WD (2001) Immunoelectron microscopy in embryos. Methods **24:** 61–69

Sierralta WD, Boenig I, Thole HH (1995) Immunogold labelling of estradiol receptor in MCF 7 cells. Cell Tissue Res **279:** 445–452

Spallarossa A, Donahue JL, Larson TJ, Bolognesi M, Bordo D (2001) *Escherichia coli* GlpE is a prototype sulfurtransferase for the single-domain rhodanese homology superfamily. Structure **9:** 1117–1125

Stoscheck CM (1990) Guide to protein purification. Methods Enzymol **182:** 50–68

Tomati U, Federici F, Canella C (1972) Rhodanese activity in chloroplasts. Physiol Chem Phys **4:** 193–196

Vennesland B, Castric PA, Conn EE, Solomonson LP, Volini M, Westley J (1982) Cyanide metabolism. Fed Proc **41:** 2639–2648

Westley J (1973) Rhodanese. Adv Enzymol Relat Areas Mol Biol **39:** 327–368

Yang SH, Berberich T, Miyazaki A, Sano H, Kusano T (2003) *NtDin,* a tobacco senescence-associated gene, is involved in molybdenum cofactor biosynthesis. Plant Cell Physiol **44:** 1037–1044